nuclear shadowing in a holographic framework

based on

L. Agozzino, P. Castorina, PC: PRL 112 (2014) 141601
EPJ C 74 (2014) 2428

Pietro Colangelo
INFN – Bari – Italy

Gauge/Gravity Duality, GGI, 13 April 2015

a comparison of
the holographic approach to data

the analysis provides an insight into some
experimental results

nuclear versus nucleon structure functions

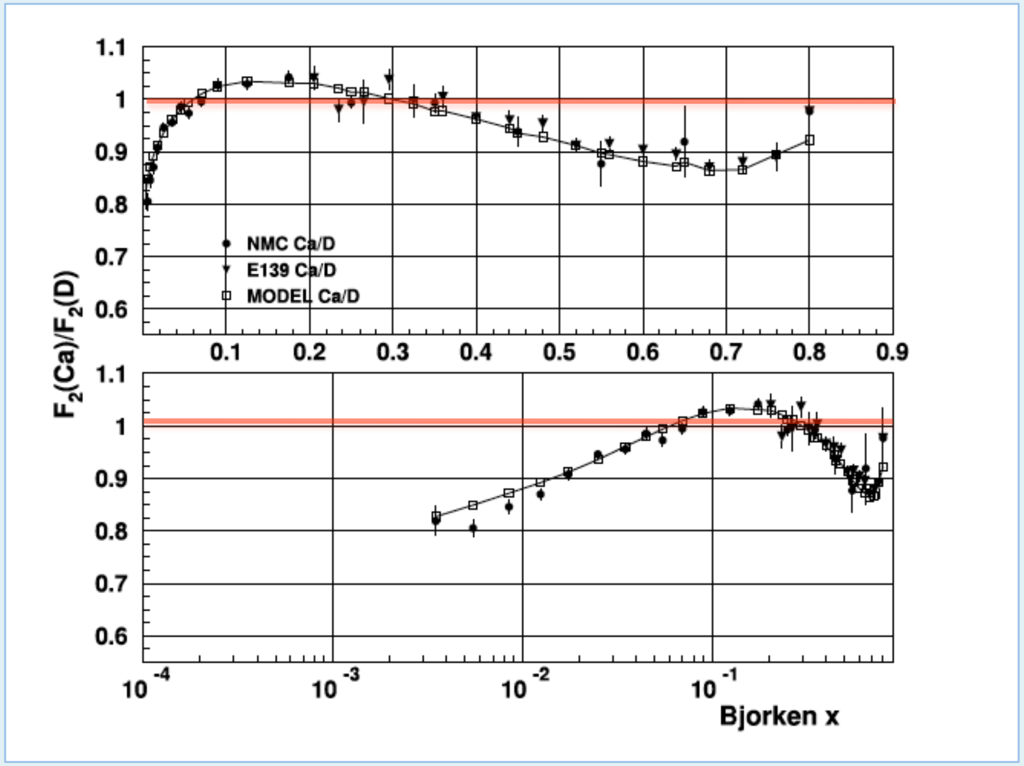

$$\frac{F_2(Ca)}{F_2(D)}$$

Kulagin and Petti, NPA 765 (2006) 126

nuclear vs nucleon structure functions

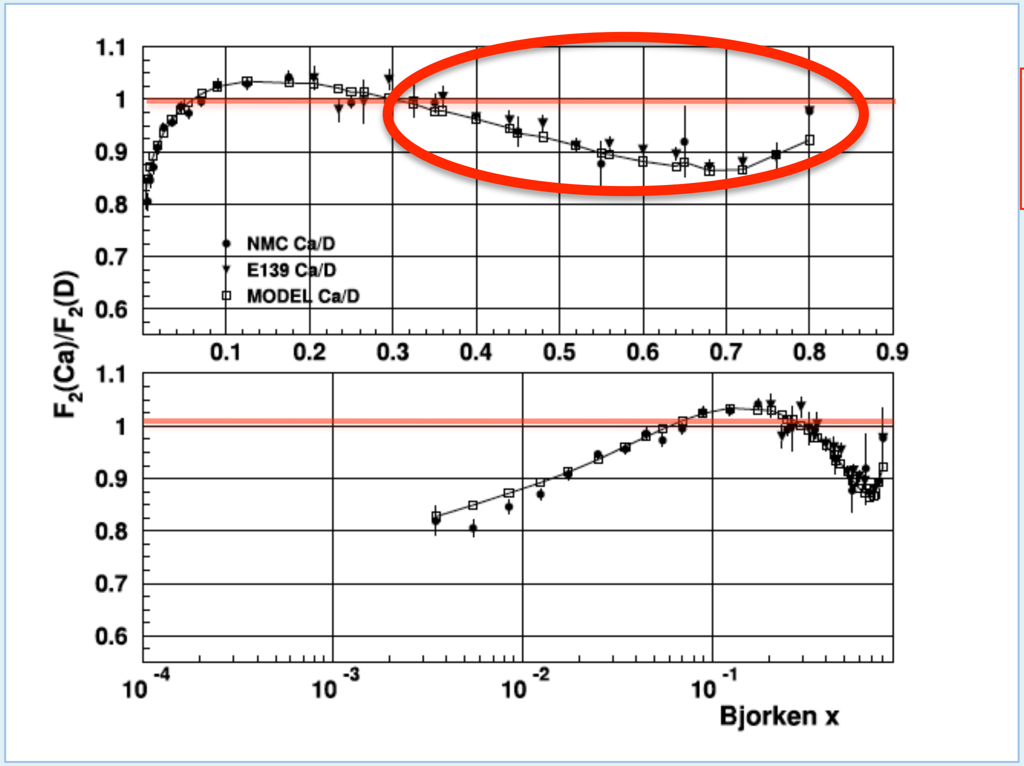

$$\frac{F_2(Ca)}{F_2(D)} < 1$$

Kulagin and Petti, NPA 765 (2006) 126

nuclear vs nucleon structure functions

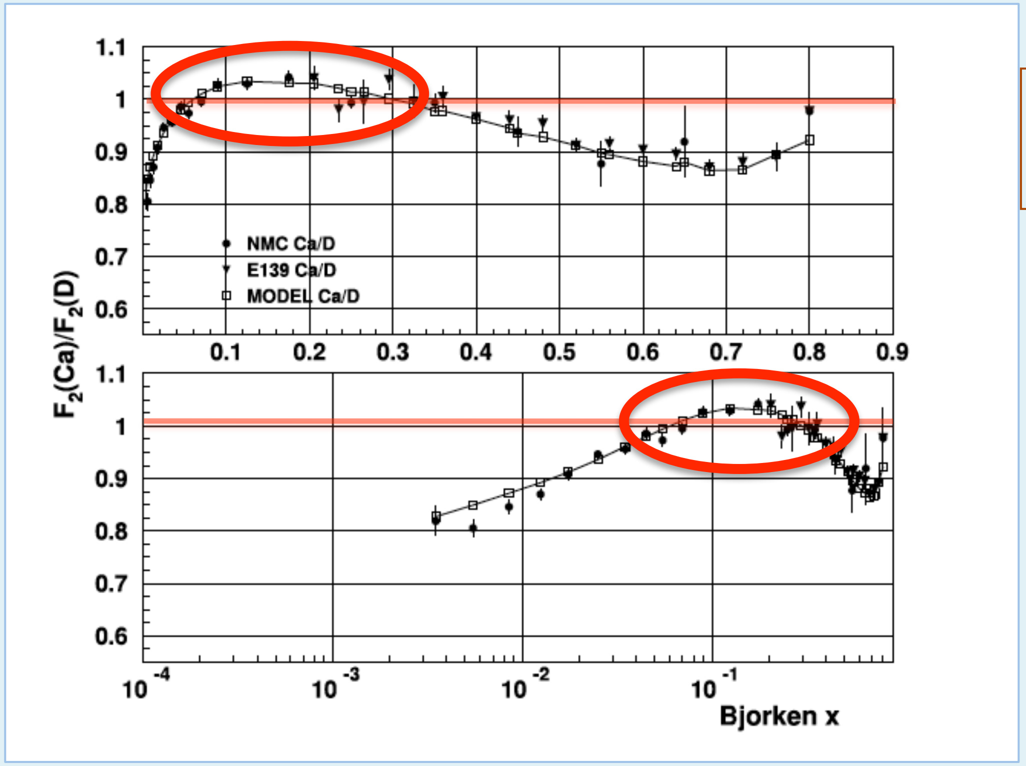

$$\frac{F_2(Ca)}{F_2(D)} > 1$$

Kulagin and Petti, NPA 765 (2006) 126

nuclear vs nucleon structure functions

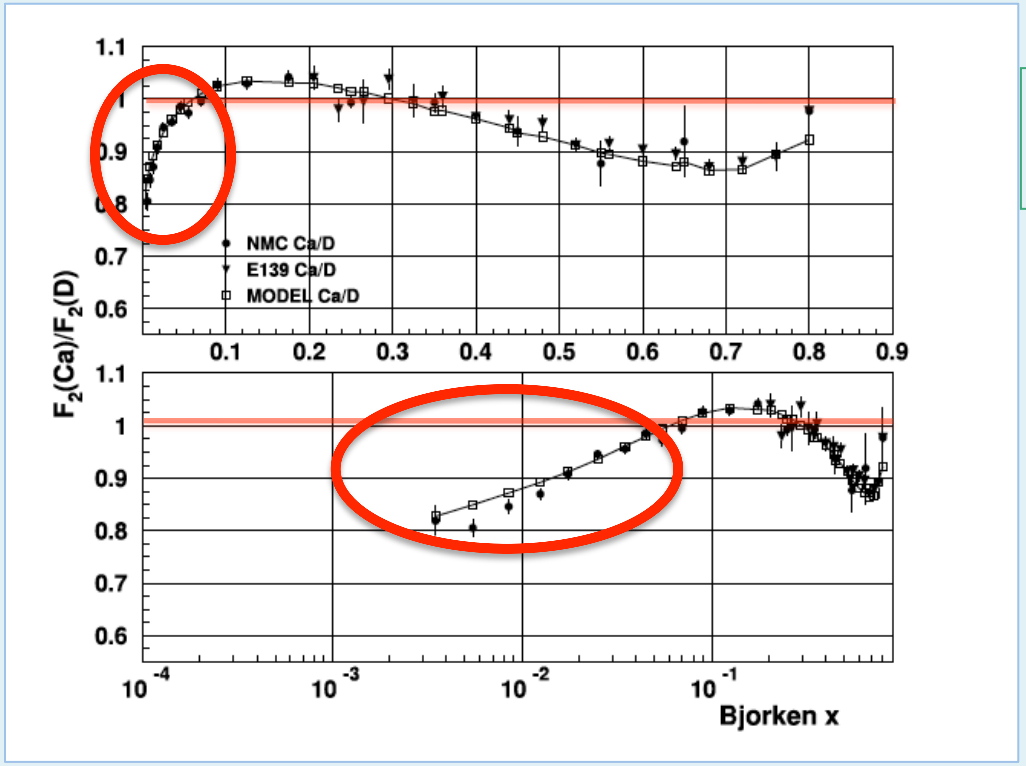

$$\frac{F_2(Ca)}{F_2(D)} < 1$$

Kulagin and Petti, NPA 765 (2006) 126

small-x domain of interest here

SUMMARY

- DIS IN QCD AND IN A STRONGLY COUPLED THEORY
- SMALL X
- ANALYSIS OF NUCLEAR DATA
- CONCLUSIONS

PROLOGUE

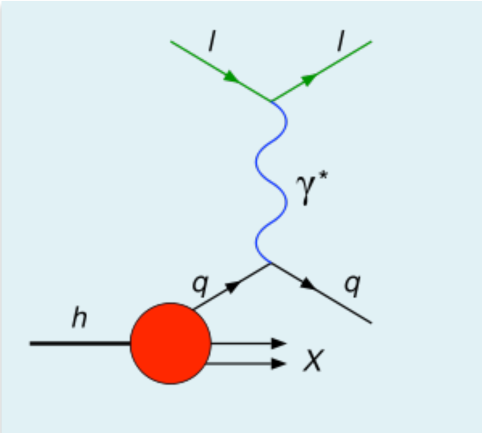

$$\frac{d^2\sigma}{dE'd\Omega} = \frac{e^4}{16\pi^2 Q^4}\left(\frac{E'}{ME}\right)\ell_{\mu\nu}W^{\mu\nu}(p,q)$$

$$W_{\mu\nu} = F_1(x,q^2)\left(\eta_{\mu\nu} - \frac{q_\mu q_\nu}{q^2}\right) + \frac{2x}{q^2}F_2(x,q^2)\left(P_\mu + \frac{q_\mu}{2x}\right)\left(P_\nu + \frac{q_\nu}{2x}\right)$$

$$Q^2 = -q^2$$

$$0 \le x = \frac{Q^2}{2\,p\cdot q} \le 1$$

Bjorken x

$F_{1,2}$ encode information on the structure of the target

PROLOGUE

DIS amplitudes from the imaginary part of the forward Compton scattering

$$T_{\mu\nu} = i\int d^4y\, e^{iq\cdot y} \langle P\tilde{Q}|T[J_\mu(y)J_\nu(0)]|P\tilde{Q}\rangle$$

$$T_{\mu\nu} = \tilde{F}_1(x,\frac{q^2}{\Lambda^2})\left(\eta_{\mu\nu} - \frac{q_\mu q_\nu}{q^2}\right) + \frac{2x}{q^2}\tilde{F}_2(x,q^2)\left(P_\mu + \frac{q_\mu}{2x}\right)\left(P_\nu + \frac{q_\nu}{2x}\right)$$

large Q^2, x>>1 : OPE for $T_{\mu\nu}$ in terms of operators $O_{n,j}$ (n=spin)

$\Delta_{n,j}=\delta_{n,j}+\gamma_{n,j}$ total scaling dimension

$\tau_{n,j}=\Delta_{n,j} - n$ twist

$$\tilde{F}_s\left(x,q^2\right) \approx i\sum_n\sum_j C^{(s)}_{n,j}A_{n,j}x^{-n}(2x)^{s-1}\left(\frac{\Lambda^2}{Q^2}\right)^{\frac{1}{2}\tau_{n,j}-1} \qquad (s=1,2)$$

large Q^2 : dominance of the operators with smallest twist

contour argument relates large x behaviour to the moments of the DIS structure functions

DIS and gauge/string duality

Polchinski Strassler JHEP 035 (2003) 012

Large ‘t Hooft coupling: gauge theories with dual description

conformal theories -> AdS$_5$ x W $\quad ds^2 = \frac{r^2}{R^2}\eta_{\mu\nu}dy^\mu dy^\nu + \frac{R^2}{r^2}dr^2 + R^2 d\hat{s}_W^2$

confining theories -> geometry modified at $\quad r \approx r_0 = \Lambda R^2$

$$\mathrm{Im}\ T_{\mu\nu} = \pi \sum_{P_X, X} \langle P,Q | J_\nu(0) | P_X, X \rangle \langle P_X, X | \tilde{J}_\mu(q) | P,Q \rangle$$

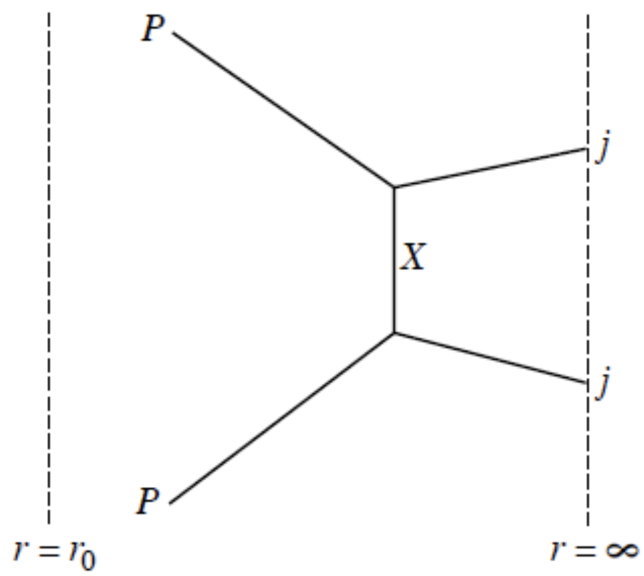

DIS and gauge/string duality

Polchinski Strassler JHEP 035 (2003) 012

Large ‘t Hooft coupling: gauge theories with dual description

conformal theories -> AdS_5 x W $\quad ds^2 = \frac{r^2}{R^2}\eta_{\mu\nu}dy^\mu dy^\nu + \frac{R^2}{r^2}dr^2 + R^2 d\hat{s}_W^2$

confining theories -> geometry modified at $\quad r \approx r_0 = \Lambda R^2$

$$\mathrm{Im}\, T_{\mu\nu} = \pi \sum_{P_X, X} \langle P,Q | J_\nu(0) | P_X, X \rangle \langle P_X, X | \tilde{J}_\mu(q) | P,Q \rangle$$

Initial/final hadron

$\Phi = e^{iPy}\psi(r,\Omega)$

normalizable mode in AdS_5 x W

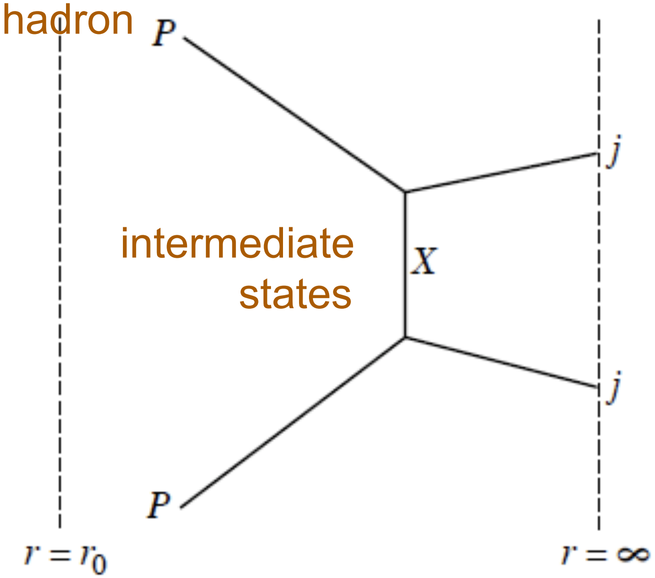

current coupling to hadron

non-normalizable mode

$$A_\mu = n_\mu e^{iqy} \frac{qR^2}{r} K_1\left(\frac{qR^2}{r}\right)$$

$$A_r = iq \cdot n\, e^{iqy} \frac{R^4}{r^3} K_0\left(\frac{qR^2}{r}\right)$$

$$q = \sqrt{Q^2}$$

DIS and gauge/string duality

Polchinski Strassler JHEP 035 (2003) 012

$$F_1 = 0 \qquad F_2 = \pi A_0 \tilde{Q}^2 \left(\frac{\Lambda^2}{Q^2}\right)^{\Delta-1} x^{\Delta+1}(1-x)^{\Delta-2}$$

scalar hadrons

Δ dimension of the local operator creating the initial/final state from the vacuum

$$F_2 = 2F_1 = \pi A_0^{'} \tilde{Q}^2 \left(\frac{\Lambda^2}{Q^2}\right)^{\tau-1} x^{\tau+1}(1-x)^{\tau-2}$$

spin 1/2 $\qquad \left(\tau = \Delta - \frac{1}{2}\right)$

emergence of 5D AdS

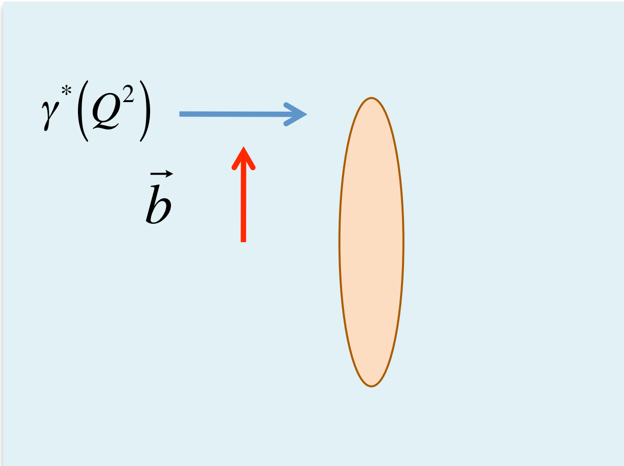

kinematical parameters:

2d Longitudinal $\quad p_0 \pm p_3 \cong \exp\left[\pm \log\left(s/\Lambda_{QCD}\right)\right]$

2d Transverse $\quad \vec{b} = \vec{x}_{perp} - \vec{x}'_{perp}$

1 Resolution $\quad z = 1/Q$

Small-x
Regge region

Pomeron contribution

$s >> \Lambda^2_{QCD}$ $\quad |t| \approx \Lambda^2_{QCD}$

$x \approx \frac{Q^2}{s}$

Regge diffusion impact parameter

$$A(s,t) \approx s^{\alpha(t)} = s^{\alpha' t + j_0} \rightarrow a(s,b_{perp}) \approx s^{j_0} \exp\left[-b^2_{perp} / 4\alpha' \log(s)\right]$$

diffusion in transverse b (impact) space

"time"=rapidity

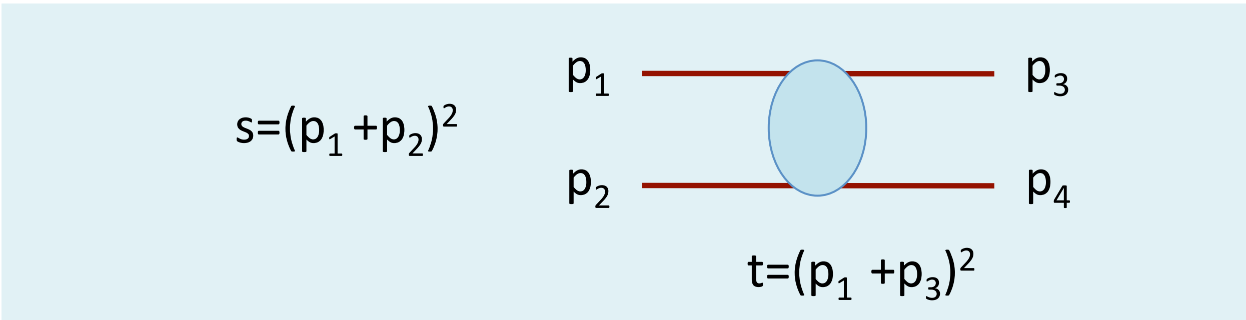

$$A\left(s,t=-q^2_{perp}\right) = \int \frac{d^2 b_{perp}}{4\pi^2} e^{-iq_{perp}\cdot b_{perp}} a\left(s,b_{perp}\right)$$

bare Pomeron

leading 1/N term exchange with cylinder topology

weak: two gluons

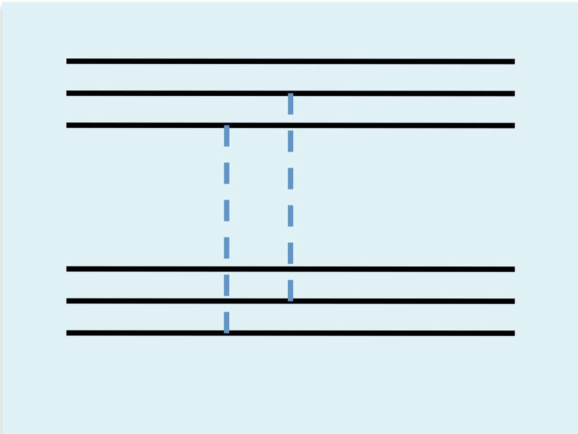

strong: AdS graviton

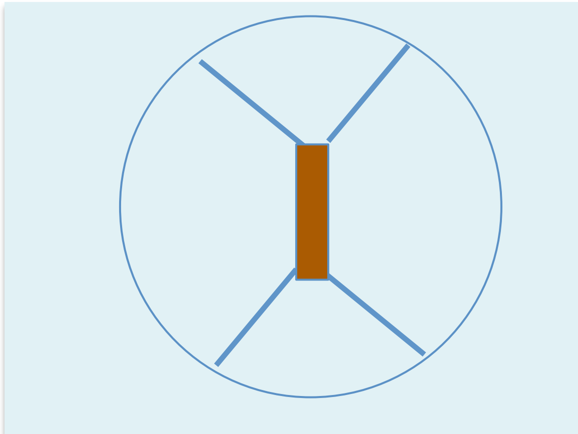

Low, PRD12 (1975) 163
Nussinov, PRL 34 (1975) 1286

Witten
Adv.Theor.Math.Phys 2 (1998) 253

BFKL Pomeron

Balitsky Fadin Kuraev Lipatov

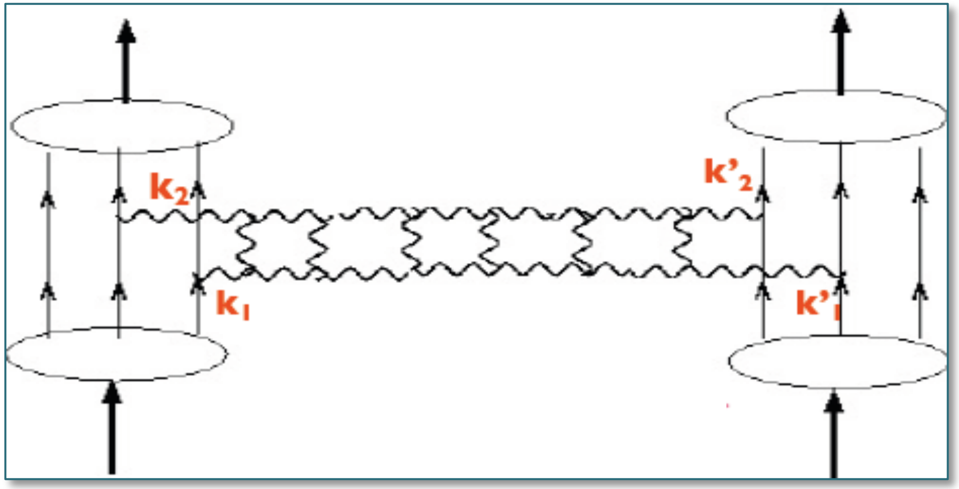

first order in λ and all orders in $(g^2 N_c \log s)^n$

“hard” Pomeron

DIS at small-x and gauge/string duality

Brower Djuric Sarcevic Tan JHEP 11 (2010) 051

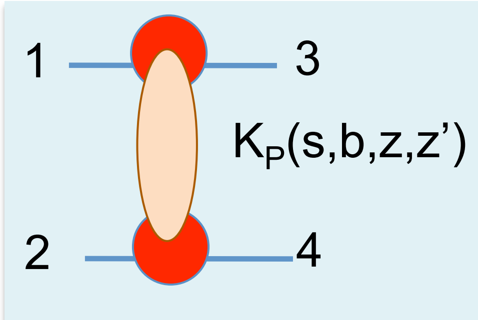

A,B -> C,D
1,2 -> 3,4

$$A(s,t) = P_{13} * K_P * P_{24}$$

scattering in 3-d transverse Euclidean AdS_3

$$A(s,t) = 2is \int d^2b\, e^{iq\cdot b} \int dz \int dz' P_{13}(z) P_{24}(z') \left\{1 - e^{i\chi(s,b,z,z')}\right\}$$

$$P_{ij}(z) = \sqrt{g}\left(\frac{z}{R}\right)^2 \phi_i^p(z)\phi_j^p(z)$$ ϕ_i external normalizable wf

$\chi(s,b,z,z')$ eikonal
related to the BPST Pomeron kernel

$$\chi(s,b,z,z') = \frac{g_0^2}{2s}\left(\frac{R^2}{zz'}\right)^2 K(s,b,z,z')$$

BPST= Brower Polchinski Strassler Tan JHEP 12 (2007) 005

DIS at small-x and gauge/string duality

Brower Djuric Sarcevic Tan JHEP 11 (2010) 051

A,B -> C,D
1,2 -> 3,4

γ* p -> γ* p
1, 2 -> 3, 4

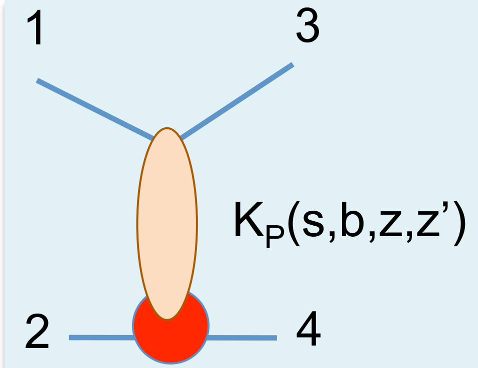

small-x DIS structure functions from the off-shell γ*p total cross section

$$F_2(x,Q^2) = \frac{Q^2}{4\pi^2\alpha_{em}}(\sigma_T + \sigma_L)$$

$$F_2(x,Q^2) = \frac{Q^2}{2\pi}\int d^2b \int dz \int dz' P_{13}(z,Q^2) P_{24}(z') \mathrm{Re}\left\{1 - e^{i\chi(s,b,z,z')}\right\}$$

$$P_{13}(z) = \frac{1}{z}(Qz)^2\left(K_0^2(Qz) + K_1^2(Qz)\right)$$

$$2xF_1(x,Q^2) = \frac{Q^2}{2\pi}\int d^2b \int dz \int dz' P_{13}(z,Q^2) P_{24}(z') \mathrm{Re}\left\{1 - e^{i\chi(s,b,z,z')}\right\}$$

$$P_{13}(z) = \frac{1}{z}(Qz)^2 K_1^2(Qz)$$

DIS at small-x and gauge/string duality

Brower Djuric Sarcevic Tan JHEP 11 (2010) 051

A,B -> C,D
1,2 -> 3,4

$\Rightarrow$

γ^* p -> γ^* p
1, 2 -> 3, 4

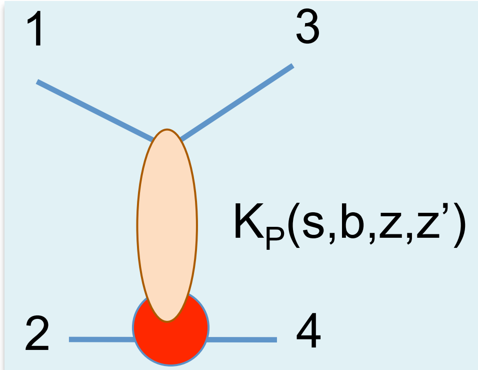

small-x DIS structure functions from the off-shell γ^*p total cross section

kernel K_P splitted in two contributions

$$F_2(x,Q^2) = F_{2,cr}(x,Q^2) + F_{2,ct}(x,Q^2)$$

DIS at small-x and gauge/string duality

Brower Djuric Sarcevic Tan JHEP 11 (2010) 051

conformal term

$$F_{2,cr}^{p}(x,Q^2) = \frac{g_0^2 \rho^{3/2}}{32\pi^{5/2}} \int dz \int dz' \frac{zz' Q^2}{\tau^{1/2}} P_{13}(z,Q^2) P_{24}(z') e^{(1-\rho)\tau} e^{\Phi(z,z',\tau)}$$

$$\Phi(z,z',\tau) = -\frac{(\log z - \log z')^2}{\rho\tau}$$

$$\tau = \log(\rho z z' s/2)$$

$$x \approx \frac{Q^2}{s}$$

g_0 ρ parameters

DIS at small-x and gauge/string duality

Brower Djuric Sarcevic Tan JHEP 11 (2010) 051

confinement term

$$F^{p}_{2,ct}(x,Q^2) = \frac{g_0^2 \rho^{3/2}}{32\pi^{5/2}} \int dz \int dz' \frac{zz' Q^2}{\tau^{1/2}} P_{13}(z,Q^2) P_{24}(z') e^{(1-\rho)\tau} e^{-\frac{\ln^2(zz'/z_0^2)}{\rho\tau}} G(z,z',\tau)$$

$$G(z,z',\tau) = 1 - 2\sqrt{\pi\rho\tau}\, e^{\eta^2} erfc(z)$$

$$\eta = \frac{-\log\left(zz'/z_0^2\right) + \rho\tau}{\sqrt{\rho\tau}}$$

z_0 IR cutoff (hard wall)

conformal term

$$F^{p}_{2,cr}(x,Q^2) = \frac{g_0^2 \rho^{3/2}}{32\pi^{5/2}} \int dz \int dz' \frac{zz'Q^2}{\tau^{1/2}} P_{13}(z,Q^2) P_{24}(z') e^{(1-\rho)\tau} e^{\Phi(z,z',\tau)}$$

local approximation

$$P_{13}(z) = \frac{1}{z}(Qz)^2\left(K_0^2(Qz) + K_1^2(Qz)\right) \rightarrow C\delta\left(z - \frac{1}{Q}\right)$$

$$P_{24}(z') \cong \delta\left(z' - \frac{1}{Q'}\right)$$

$$F^{p}_{2,cr}(x,Q^2,Q') = \frac{g_0^2 \rho^{3/2}}{32\pi^{5/2}} \frac{Q}{Q'} \frac{1}{\tau^{1/2}} e^{(1-\rho)\tau} e^{-\left[\log^2(Q/Q')/\rho\tau\right]}$$

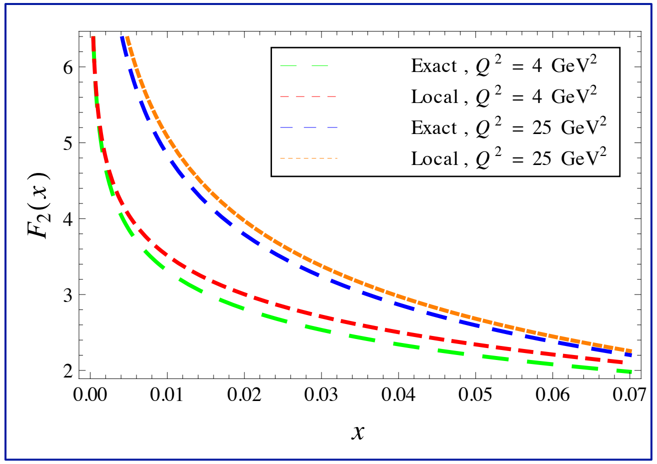

F_2^p vs $F_2^p\big|_{local}$

confinement term

$$F_{2,ct}^{p}(x,Q^2) = \frac{g_0^2 \rho^{3/2}}{32\pi^{5/2}} \int dz \int dz' \frac{zz' Q^2}{\tau^{1/2}} P_{13}(z,Q^2) P_{24}(z') e^{(1-\rho)\tau} e^{-\frac{\ln^2(zz'/z_0^2)}{\rho\tau}} G(z,z',\tau)$$

local approximation

$$P_{13}(z) = \frac{1}{z}(Qz)^2 \left(K_0^2(Qz) + K_1^2(Qz)\right) \rightarrow C\delta\left(z - \frac{1}{Q}\right)$$

$$P_{24}(z') \cong \delta\left(z' - \frac{1}{Q'}\right)$$

$$Q_0 = 1/z_0$$

$$F_{2,ct}^{p}(x,Q^2,Q',Q_0^2) = \frac{g_0^2 \rho^{3/2}}{32\pi^{5/2}} \frac{(Q/Q')}{\tau^{1/2}} e^{(1-\rho)\tau} e^{-\frac{\ln^2(Q_0^2/(QQ'))}{\rho\tau}} G\left(\frac{1}{Q}, \frac{1}{Q'}, \tau\right)$$

$$F_2^p = F_{2cr}^p + F_{2ct}^p$$

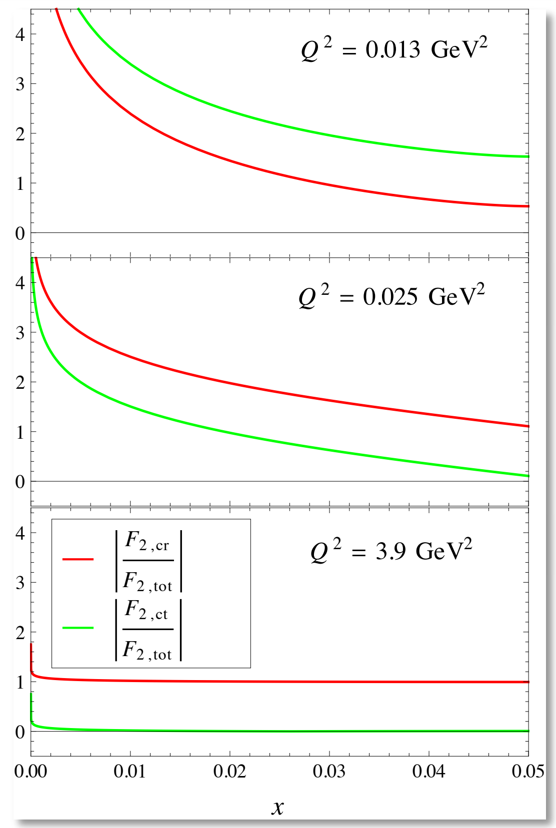

H1-ZEUS small-x measurements

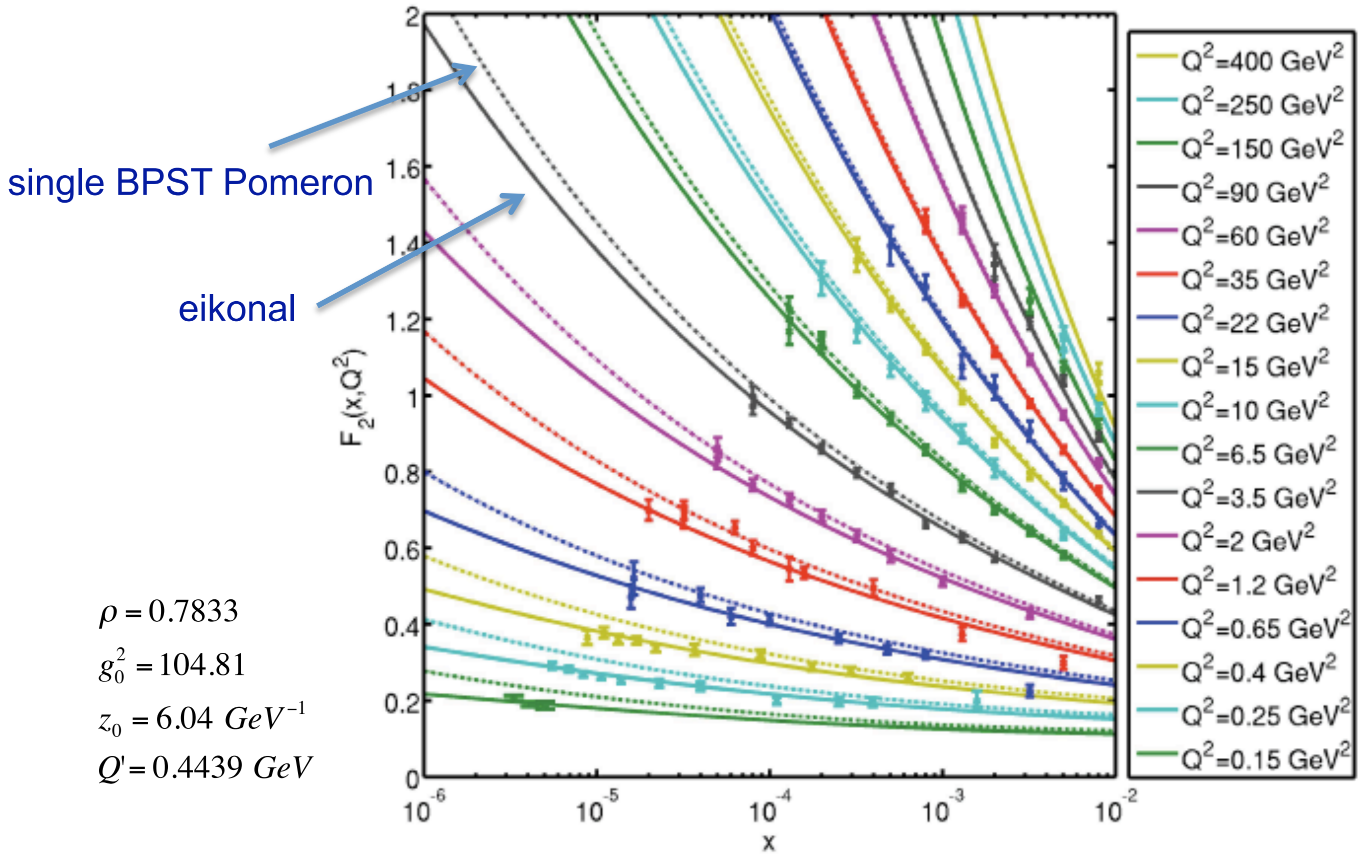

$\rho = 0.7833$

$g_0^2 = 104.81$

$z_0 = 6.04\ GeV^{-1}$

$Q' = 0.4439\ GeV$

Brower et al. 2010

good description of the data in the small-x region

inclusion of eikonal not necessary – the saturation regime is not reached

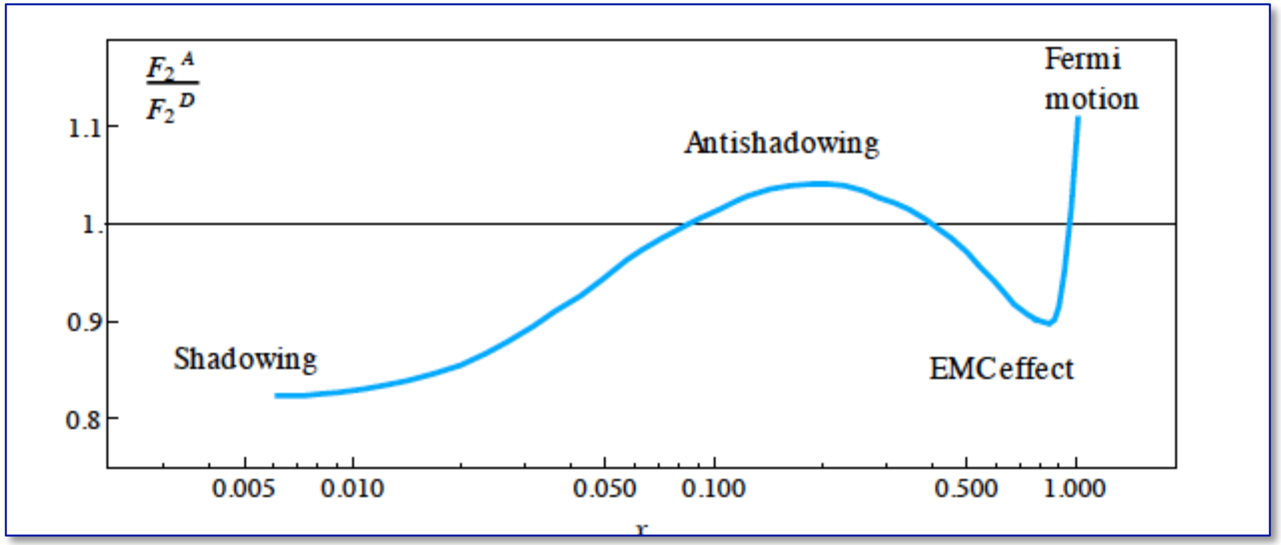

$\frac{F_2^A}{F_2^D}$
1.1
1.
0.9
0.8
Shadowing
Antishadowing
EMCeffect
Fermi
motion
0.005
0.010
0.050
0.100
0.500
1.000

isospin violation can be included in the formula for F_2

$$F_2^n = F_{2cr}^p\left(x,Q^2,Q_n^{'}\right) + F_{2ct}^p\left(x,Q^2,Q_n^{'},Q_{0n}^2\right)$$

similar proton and neutron confinement scale $Q_{0n} \cong Q_0$

experimental information from DIS on deuterium

nuclear structure function F_2 in the holographic framework

conformal term

$$F^{p}_{2cr}(x,Q^2,Q') = \frac{g_0^2 \rho^{3/2}}{32\pi^{5/2}} \frac{Q}{Q'} \frac{1}{\tau^{1/2}} e^{(1-\rho)\tau} e^{-\left[\log^2(Q/Q')/\rho\tau\right]}$$

$$Q'_A = \lambda_A Q' \Rightarrow Q^2 \to Q^2/\lambda_A^2$$

$$F_2^A(x,Q^2) = F^N_{2cr}\left(x, \frac{Q^2}{\lambda_A^2}, Q'\right)$$

peak of the wave function
of the bound nucleon

confinement term

$$F^{p}_{2ct}(x,Q^2,Q') = \frac{g_0^2 \rho^{3/2}}{32\pi^{5/2}} \frac{Q}{Q'} \frac{1}{\tau^{1/2}} e^{(1-\rho)\tau} e^{-\left[\log^2\left(Q_0^2/QQ'\right)/\rho\tau\right]} G\left(\frac{1}{Q}, \frac{1}{Q'}, \tau\right)$$

$$Q'_A = \lambda_A Q' \Rightarrow Q_0^2 \to Q_0^2/\lambda_A^2$$

Q^2 rescaling rule:

$$F_2^A(x,Q^2) = F^N_{2cr}\left(x, \frac{Q^2}{\lambda_A^2}, Q'\right) + F^N_{2ct}\left(x, \frac{Q^2}{\lambda_A^2}, Q', \frac{Q_0^2}{\lambda_A^2}\right)$$

deuterium structure function

$$F_2^{D} = \frac{1}{2}\left[F_2^{pD} + F_2^{nD}\right]$$

$$F_2^{pD} = F_2^{p}\left(x, \frac{Q^2}{\lambda_D^2}, Q', \frac{Q_0^2}{\lambda_D^2}\right)$$

$$F_2^{nD} = F_2^{n}\left(x, \frac{Q^2}{\lambda_D^2}, Q'_n, \frac{Q_0^2}{\lambda_D^2}\right)$$

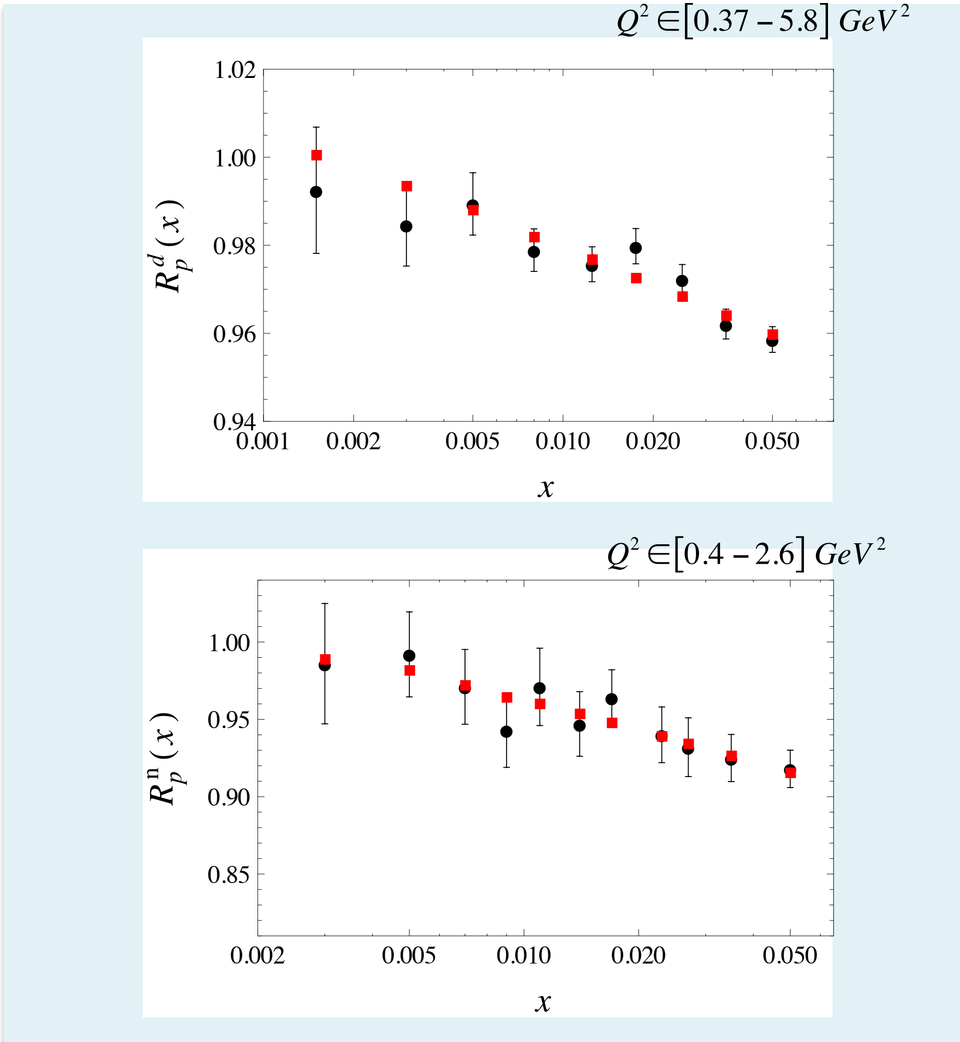

our model

New Muon Collaboration (CERN)
NPB 487 (1997) 3
NPB 371 (1992) 3

nuclear structure function F_2

nucleus	data set
He	9
Li	9
Be	6
C	15
Al	6
Ca	9
Fe	6
Pb	6

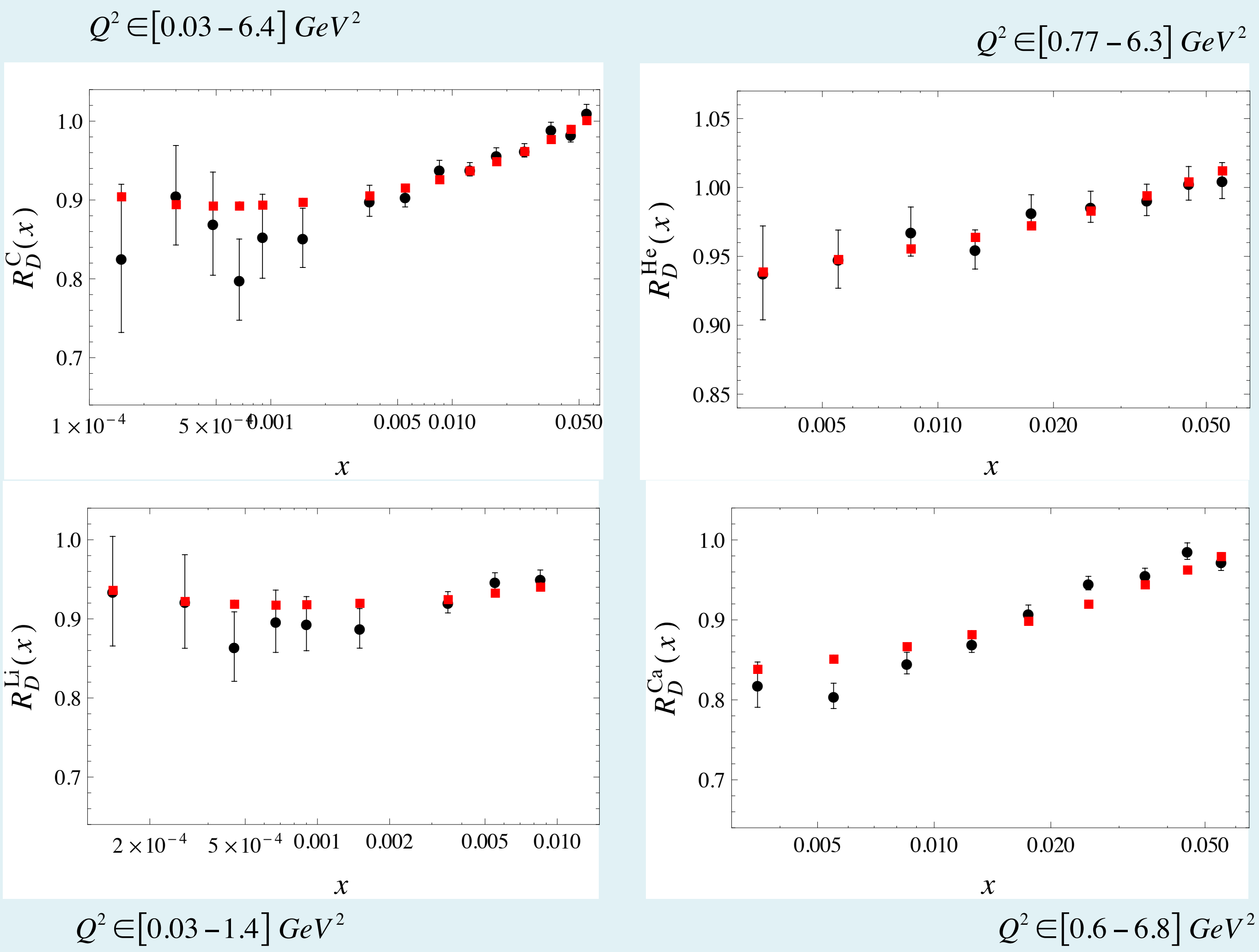

$$R_D^A = \frac{F_2^A}{F_2^D}$$

our model

New Muon Collaboration
PLB 441 (1995) 3, NPB 441(1995) 12
NPB 481 (1996) 3

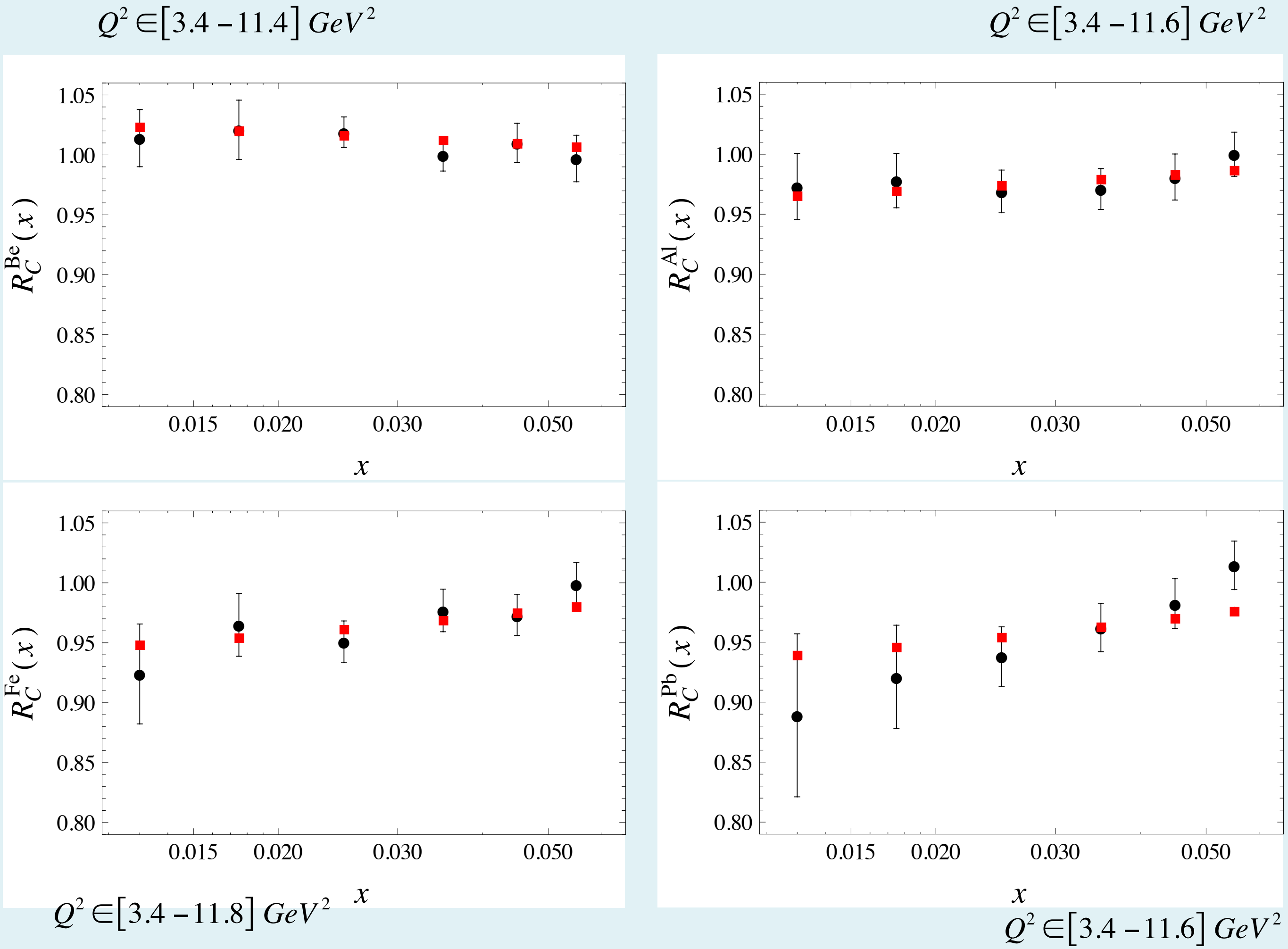

$$R_C^A = \frac{F_2^A}{F_2^C}$$

our model

New Muon Collaboration
PLB 441 (1995) 3, NPB 441(1995) 12
NPB 481 (1996) 3

nucleus	n. points	$\chi^2_{d.o.f}$	n. points	$\chi^2_{d.o.f}$	range of $\langle Q^2 \rangle$
He	9	1.09	9	0.24	[0.77 – 6.3]
Li	9	0.93	9	0.79	[0.03 – 1.4]
Be	6	0.21	6	0.30	[3.4 – 11.4]
C	9	1.61	15	0.89	[0.03 – 6.4]
Al	6	0.23	6	0.21	[3.4 – 11.6]
Ca	9	8.0	9	3.87	[0.6 – 6.8]
Fe	6	0.41	6	0.42	[3.4 – 11.8]
Pb	6	1.11	6	0.93	[3.4 – 11.6]

Table 1 Experimental data sets [21] and $\chi^2_{d.o.f}$ of the fit of the structure function F_2^A for each nucleus. The third column reports the $\chi^2_{d.o.f}$ of fits without isospin breaking, the fourth and fifth columns correspond to fits with the isospin breaking effect included. In the last column, the experimental average Q^2 ranges (in GeV^2) for the various cases are indicated, from the first to the last bin of the Bjorken x.

Isospin effect included

$$F_2^A(x,Q^2) = \frac{Z}{A} F_{2ct}^p\left(x,\frac{Q^2}{\lambda_A^2},Q',\frac{Q_0^2}{\lambda_A^2}\right) + (1-\frac{Z}{A}) F_{2ct}^n\left(x,\frac{Q^2}{\lambda_A^2},Q_n',\frac{Q_0^2}{\lambda_A^2}\right)$$

conventional approach: QCD dipole model

γ^* produces a qq pair which interacts with the target

$$\frac{\sigma^{\gamma^* A}(\tau^A)}{\pi R_A^2} = \frac{\sigma^{\gamma^* N}(\tau^N)}{\pi R_N^2}$$

τ_A saturation scale

$$\lambda_A = \left(\frac{A R_N^2}{R_A^2} \right)^{1/2\delta}$$

$\pi R_N^2 = 1.55 \text{ fm}^2$

$\delta = 0.79$

$R_A = \left(1.12 A^{1/3} - 0.86 A^{-1/3}\right) \text{ fm}$

nucleus	λ_A (holography)	$\lambda_{A,dip}$[24]
Li	1.843	1.130
Be	1.764	1.140
C	1.775	1.160
Al	1.972	1.264
Ca	2.006	1.338
Fe	2.090	1.413
Pb	2.286	1.780

Table 2 Rescaling parameter λ_A obtained using the holographic expression for F_2^A and taking into account the isospin breaking. The values in the last column are obtained within the QCD dipole model [24].

J.L.Albacete et al
EPJ C 43 (2005) 353
PRD 71 (2005) 014003

Q^2 rescaling versus x rescaling

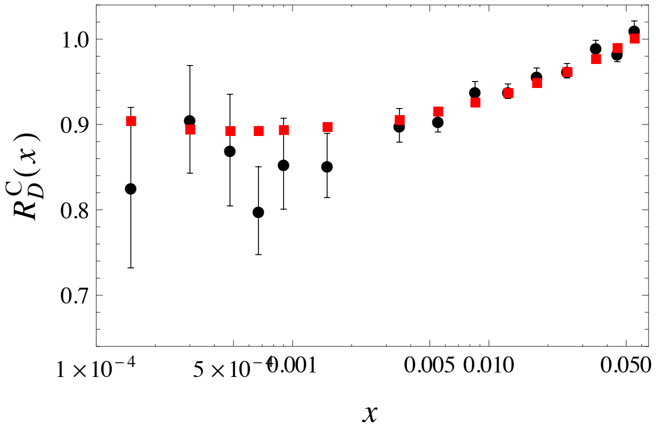

$$x \rightarrow \lambda_A \; x$$

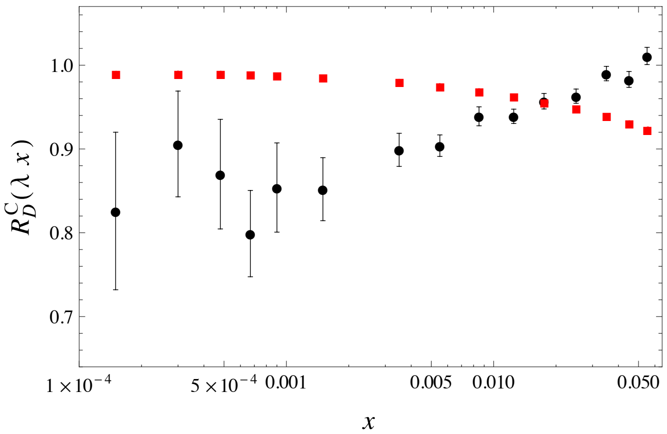

● data
■ our model

longitudinal structure function

$$F_L = F_2 - 2xF_1$$

proton

$Q^2 \in [1.5 - 45]\ GeV^2$

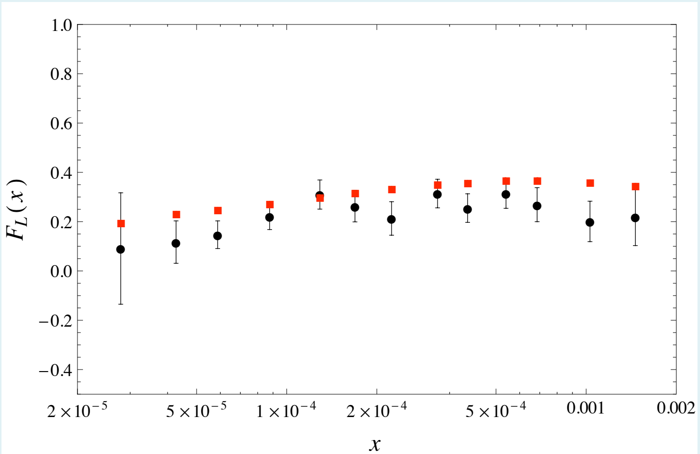

our model

H1 Collaboration
EPJ C71 (2011) 1579

nuclear modification of the longitudinal structure functions

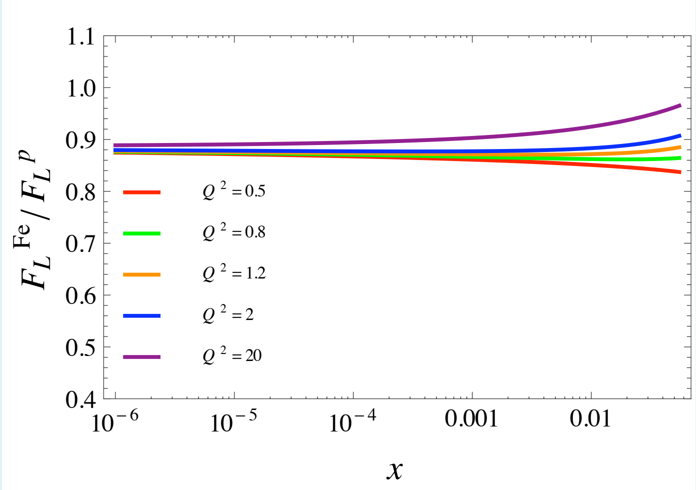

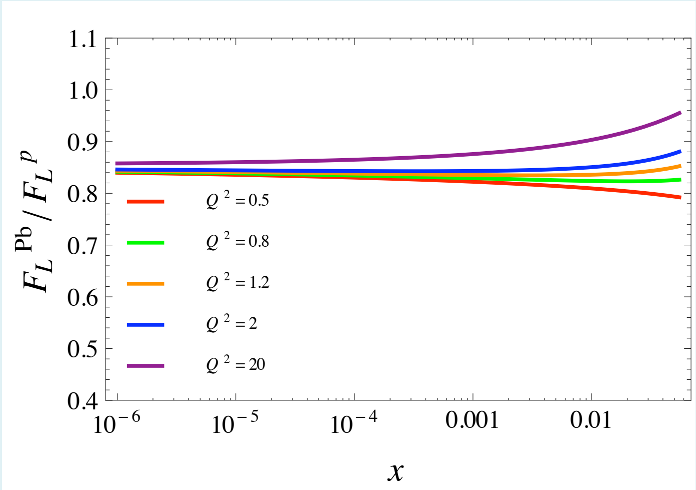

$$\frac{F_L^A}{F_L^p}$$

structure functions from cross section measurements

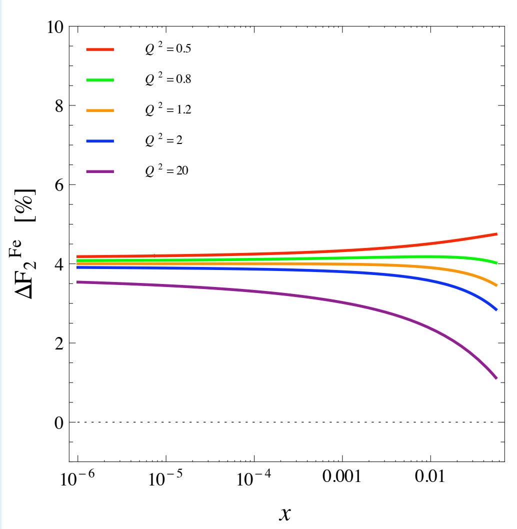

reduced cross section

$$\sigma_r = F_2 \left[1 - f(y) \frac{F_L}{F_2} \right]$$

maximum uncertainty on F_2

$$\Delta F_2 = 1 - \frac{F_2^A}{F_2^A + f(y)(F_L^N - F_L^A)}$$

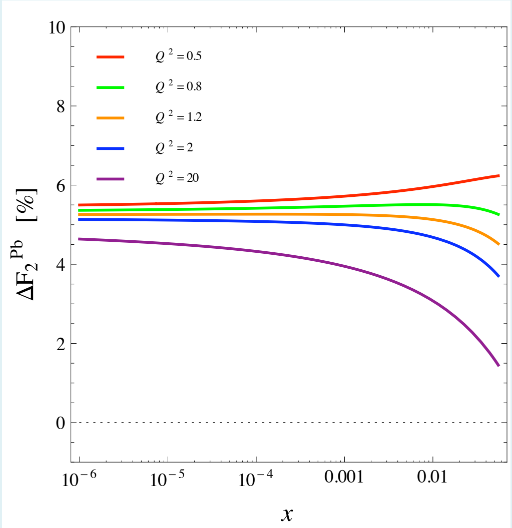

by Q^2 rescaling at low-x, the expression of F_2 obtained in the gauge/gravity formulation reproduces the set of nuclear data

rescaling can be understood in terms of a modification of the z_{IR} in nuclei and in the change of the peak of the wave function of the bound nucleon

geometrical interpretation of nuclear shadowing

Questions:

anti-shadowing by momentum rescaling?

holographic description of the EMC effect?

Anti-shadowing usually analyzed by energy-momentum sum rules

Nature of the EMC effect debated

Conclusions

A unified description of nuclear structure functions in the full x-range is missing

The gauge/gravity duality formulation seems to capture the relevant dynamics to describe nuclear DIS phenomena at small-x

Possibilities for the description of anti-shadowing and of the EMC effect need to be investigated

Interest for neutrino DIS on nuclear targets -> neutrino cross section at high energy and small-x: a definition of the charged current in the dual approach is needed

SPARES